WORKING PAPER
MANSHOLT GRADUATE SCHOOL

Minimum volume simplicial enclosure for spectral unmixing

Eligius M.T. Hendrix, Inmaculada García,
Javier Plaza and Antonio Plaza

DISCUSSION PAPER No. 50
2010

Mansholt Graduate School of Social Sciences

Hollandseweg 1, 6706 KN Wageningen,
The Netherlands
Phone: +31 317 48 41 26
Fax: +31 317 48 47 63
Internet: http://www.mansholt.wur.nl/
e-mail: office.mansholt@wur.nl

Working Papers are interim reports on work of Mansholt Graduate School (MG3S) and have received only limited reviews[1]. Each paper is refereed by one member of the Editorial Board and one member outside the board. Views or opinions expressed in them do not necessarily represent those of the Mansholt Graduate School.

The Mansholt Graduate School's researchers are based in two departments: 'Social Sciences' and 'Environmental Sciences' and two institutes: 'LEI, Agricultural Economics Research Institute' and 'Alterra, Research Institute for the Green World'. In total Mansholt Graduate School comprises about 250 researchers.

Mansholt Graduate School is specialised in social scientific analyses of the rural areas and the agri- and food chains. The Graduate School is known for its disciplinary and interdisciplinary work on theoretical and empirical issues concerning the transformation of agriculture, rural areas and chains towards multifunctionality and sustainability.

Comments on the Working Papers are welcome and should be addressed directly to the author(s).

Eligius Hendrix	Wageningen Universiteit and Universidad de Málaga, Eligius.Hendrix@wur.nl
Inmaculada García	Universidad de Almería, igarcia@ual.es
Javier Plaza	Universidad de Extremadura, jplaza@unex.es
Antonio Plaza	Universidad de Extremadura, aplaza@unex.es

[1] Working papers may have been submitted to other journals and have entered a journal's review process. Should the journal decide to publish the article the paper no longer will have the status of a Mansholt Working Paper and will be withdrawn from the Mansholt Graduate School's website. From then on a link will be made to the journal in question referring to the published work and its proper citation.

Minimum volume simplicial enclosure for spectral unmixing *

Eligius M.T. Hendrix
Wageningen University and Universidad de Málaga, Eligius.Hendrix@wur.nl

Inmaculada García
Universidad de Almería, igarcia@ual.es

Javier Plaza and Antonio Plaza
Universidad de Extremadura, jplaza@unex.es and aplaza@unex.es

We describe the minimum volume enclosing simplex problem, which is known to be a Global Optimization problem and illustrate its multimodality. The problem has been used as a basis to estimate so-called endmembers and abundance fractions in unmixing spectral data from remotely sensed hyperspectral sensors. This estimation problem is a big challenge. We explore the possibility of a new estimation algorithm using the minimum volume enclosing simplex problem. We investigate its behaviour numerically on designed instances, comparing its outcomes with a maximum volume enclosed simplex approach which is used frequently in spectral unmixing.

Key words: spectral unmixing, endmembers, princicpal components, optimization, minimum volume

1. Introduction

A challenging problem in interpreting data collected by remotely sensed hyperspectral imaging sensors is to unfold them into spectrally pure components (Adams et al. (1986)). We study here the possibility to do so using a minimum volume enclosing simplex approach. Hyperspectral sensors record scenes in which various disparate material substances contribute to the spectrum measured for a single pixel (Goetz et al. (1985), Green et al. (1998), Chang (2003)). Given such mixed pixels, one would like to identify the individual constituent materials present in the mixture, as well as the proportions in which they appear. Spectral unmixing (Keshava and Mustard (2002)) is a term to denote a procedure to decompose a measured spectrum of a mixed pixel into a collection of constituent spectra (endmembers) and a set of corresponding fractions (abundances) that indicate the proportion of each endmember present in the pixel. Endmembers normally correspond to familiar macroscopic objects in the scene, such as water, soil, metal, or any natural or man-made materials.

Many methods have been developed and tested to perform endmember extraction and unmixing, see Keshava (2003) and Plaza et al. (2004) for an overview. In practice, analyzing spectral mixtures can be complicated because of nonlinear effects observed in pixel composition and noise. We will focus on so-called linear unmixing (Heinz and Chang (2001)) and address the question of how to recover the endmember and abundance data via unbiased estimators. Notice that noise in hyperspectral imaging instruments is relatively low. Therefore, standard least squares approaches have been adopted with the additional complication that the abundance estimate should lay on the unit simplex (nonnegativity). Miao and Qi (2007) describe an approach where two conflicting objectives, that of least squares and minimizing the volume of an enclosing simplex are combined in an objective function. The original idea of using a minimum volume enclosing simplex in the field of

* This work has been supported by the Spanish Ministry of Science and Innovation through grants TIN2008-01117 and AYA2008-05965-C04-02. Eligius Hendrix is a fellow of the Spanish "Ramon y Cajal" contract program, co-financed by the European Social Fund.

remote sensing for endmember extraction, is due to Craig (1994). More recently, Chan et al. (2009) developed an approach where sequential Linear Programming is applied to solve the minimum volume enclosing simplex problem. In this paper we use standard available nonlinear optimization algorithms.

The problem of enclosing a set of points with a minimum volume body leads usually to a Global Optimization problem. We will illustrate that for the generic simplicial enclosure this is the same. However, the use of this approach in spectral unmixing is far from worst case behavior; instances are characterised by low noise and pixel data is well spread. A local search from a well designed starting body leads to the global optimum soon. We adopt a hierarchical vision: First, we minimize least squares using principal component analysis (PCA), which is very common in image data analysis (Richards and Jia (2006)) and, second, we minimize the volume of an enclosing simplex in the reduced space. The question is how to use such an approach to obtain unbiased estimates of endmembers and fractional abundances in the case of linear mixtures with white noise.

A benchmark method is to consider a maximum volume "inscribing" simplex searched for by the so-called N-FINDR algorithm extensively described in Winter (2003). Given the reduced data, in principle one looks for all combinations within the given pixels as candidate endmembers such that the resulting volume of the spanning simplex is maximum. If indeed the endmembers are present in the data and noise is low, the approach is very promising as analysed in Winter (2003). We can use the results of such an approach to compare methods numerically.

The remainder of the paper is organized as follows. In Section 2, we describe the estimation problem under consideration. Section 3 gives the minimum volume enclosing simplex problem and illustrates its multimodal character. In Section 4, a new procedure is developed and the N-FINDR algorithm is sketched. Section 5 illustrates with numerical instances the feasibility of the approach. Finally, conclusions and hints at plausible future research are given in Section 6.

2. Unmixing and minimum enclosing simplex

We describe the linear unmixing problem using the following notation throughout:

Indices

- i index of band, $i = 1, \ldots, m$
- j index of endmember $j = 1, \ldots, n$
- k index for pixel $k = 1, \ldots, r$

Assumed model

$$y = Xa + \varepsilon \tag{1}$$

where y is an $m \times 1$ observed pixel vector, X is an $m \times n$ matrix of endmembers, a is an $n \times 1$ abundance vector and ε is an $m \times 1$ white noise vector with a standard deviation of σ.

The question is how to recover "real" matrix X and abundance a_k of observed pixels k. To do so, usually two objectives are minimized: noise (in a least squares sense) and the volume of the simplex spanned by the columns of matrix X. Moreover, the abundance should be positive for each pixel in the given data $Y = y_1, \ldots, y_k, \ldots, y_r$. Another question is how to deal with least squares and minimum volume in such a way that the estimation is unbiased, i.e. the expected value of the estimator is the real value. This is more or less a statistical question. Literature on unmixing handles the question usually from an algorithmic perspective (Plaza et al. (2004)). Are the resulting images of the so-called abundance maps that depict the value of abundance a_j for each constituent j in all the pixels "close to" that of the input image? This is not a hard criterion, but provides the opportunity to depict the real result. One should keep in mind that instances of the problem consisting of real images are characterized by pixels being mixtures of generally less than 4–5 constituents, i.e. the vector a has only a few positive values. Moreover, sensor noise is relatively low.

The idea of least squares in the estimation procedure relies on the fact that, often, the number of endmember constituents is not known. Therefore, application of PCA is a useful approach. Assuming

n endmembers means that one should discover an $n-1$ dimensional subspace that is responsible for the main variation, while the rest of the m dimensional space is considered noise.

First of all the data are centralized by the mean $\overline{y}$, such that the columns of Y consist of centralized observations $y_k - \overline{y}$. The observed variation in the spectral data Y^TY is approximated by $(CZ)^TCZ$ where C is an $m \times (n-1)$ matrix of principal components and Z is $(n-1) \times r$ a so-called score matrix. In direction c_1 we have the biggest variation, in direction c_2 the second biggest, etc. Essentially we have reduced model (1) to

$$z = Va + \xi, \tag{2}$$

where we expect the endmembers X to lay in the space $< C > + \overline{y}$ spanned by the columns of C. We should keep in mind that C represents an estimate of the space in which the endmember spectra X are located, $X = CV + \overline{y}$. To put it in another way, with absense of noise the estimate of C represents the space spanned by $X - \overline{y}\mathbf{1}^T$, where $\mathbf{1}$ is the all-ones vector of appropriate dimension. With noise, ξ is now the projection of ε on $< C >$ and therefore its components also form white noise. To be consistent, we should theoretically notice that $y = Cz + \overline{y} + \zeta$ where ζ is the part of ε projected on the orthoplement of $< C >$; $\varepsilon = \xi + \zeta$. From these detailed statistical observations we will use the idea that the noise of z is componentwise independent.

Miao and Qi (2007) present an elegant matrix factorisation approach. They simultaneously minimize least squares and the simplex volume. These objectives are conflicting. For volume reduction it is good to add a direction without variation to the principal components; zero variation gives zero volume. The least squares idea gives that we look for directions with maximum variation.

In this work, we follow a two-step approach often found in literature. First we estimate the space in which the n endmembers are lying. Secondly, in that space, we minimize the volume of a simplex such that it encloses the projections of the observed bands of the pixels. The N-FINDR algorithm follows an approach where the volume of a simplex is maximized on the projected plane. In the following section, we focus on these two approaches and compare them further.

3. Minimum volume versus maximum volume simplices

The estimate of the matrix of endmembers $X = CV + \overline{y}$ appears from an estimate of V based on the projected bands (scores) Z. We first focus on the minimum volume enclosing simplex problem and then show its relation with the maximum volume approach of the N-FINDR method. The problem of finding the minimim volume enclosing simplex of a set of points $z_k, k = 1, \ldots, r$ in $(n-1)$-dimensional space is

$$\min_V \{f(V) := \det \begin{pmatrix} V \\ \mathbf{1}^T \end{pmatrix}\} \tag{3}$$

subject to

$$a_k = \begin{pmatrix} V \\ \mathbf{1}^T \end{pmatrix}^{-1} \begin{pmatrix} z_k \\ 1 \end{pmatrix} \geq 0, \quad k = 1, \ldots, r \tag{4}$$

where $\mathbf{1}$ is the all-ones vector.

Enclosing a set of points with shapes has specific mathematical characteristics. For any convex shape where one minimizes the volume, the points in the interior of the convex hull do not matter. However, the determination of points on the boundary and in the interior of the convex hull is as hard to determine as the minimum volume shape. Moreover, the number of active points on the boundary of the minimum volume shape is limited. Hendrix and Toth (2010) give several examples for enclosing with spheres (the Chebychev problem) and with hyper-rectangles.

The next property to discuss is that we are dealing with a Global Optimization problem. This is a general characteristic of minimizing the volume of enclosing shapes and maximizing the volume of enclosed shapes. Enclosing a set of points by a minimum sphere is a convex problem and therefore relatively easy to solve. Khachiyan and Todd (1993) and Sun and Freund (2004) discuss for instance

the complexity of enclosing and enclosed ellipsoids. Hendrix and Toth (2010) use a small instance with only 4 points to illustrate the complexity of the enclosing hyperrectangle problem. We follow the same approach for the minimum volume enclosing simplex problem.

EXAMPLE 1. Given matrix of points $Z = \begin{pmatrix} 0 & 4 & 4 & 1 \\ 0 & 0 & 4 & 4 \end{pmatrix}$. Problem (3) has several local minima for this instance. Moreover, the global minimum solution is not unique. In Figure 1, three enclosing simplices are given. Vertex matrices $\begin{pmatrix} 0 & 6 & 2 \\ 0 & 0 & 8 \end{pmatrix}, \begin{pmatrix} -2 & 4 & 4 \\ 0 & 0 & 8 \end{pmatrix}$ give volume 48 and $\begin{pmatrix} -2 & 6 & 2 \\ 4 & 4 & -4 \end{pmatrix}$ represents a simplex of volume 64. The latter is called a local minimum solution as moving the vertices a bit such that it still encloses the points increases its volume. Further analysis shows that the number of global minimum solutions is infinite.

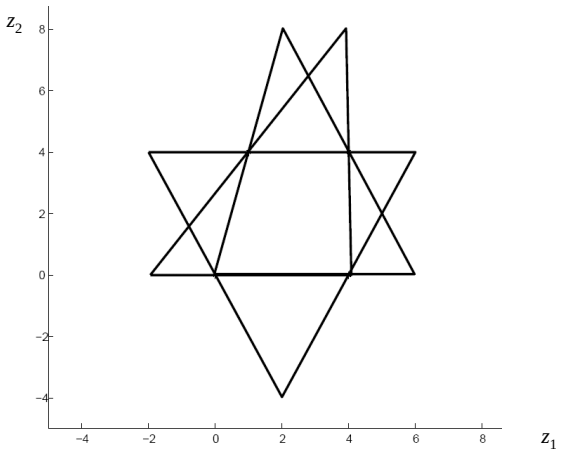

Figure 1 Three enclosing simplices of 4 pixels. Two have a minimum volume. The other is a local nonglobal solution

First of all one should keep in mind that the set of global optimum solutions of (3) and (4) contains $n!$ solutions as any permutation of the columns in V represents the same solution. It is usual in spectral unmixing that one has to allocate the endmembers to the constituents during an interpretation of estimation results. Besides symmetry, generic problem (3) may be hard when we think of a "round" cloud of points as in Example 1. To illustrate bad case behaviour we construct an instance where the points are distributed over the unit ball.

EXAMPLE 2. To give a good picture of mutimodality is not straightforward; even in the 2-dimensional cases the minimum simplicial volume problem has 6 parameters to optimize. Therefore we construct a parametrized example where the angle of the first edge α of the simplex is fixed and we optimize over the other parameters as illustrated in Figure 2. The basis of the bad case is enclosing the unit ball (any ellips also would do) with a (regular) simplex of volume $3\sqrt{3} \approx 5.2$. For the illustration we generate 10 points over the unit ball and solve problem (3), (4) fixing α and the corresponding edge minimizing over the rest of the parameters. The result of this exercise is Figure 3 which shows the minimum volume varying the value of α. The visible local minima are local minima of problem (3), (4). The instance shows that the number of optima when points z_k are 2-dimensional increases with the number r of points as long as they are in the convex hull. This is confirmed by findings of Zhou and Suri (2002) who construct a specific algorithm for 3-dimensional instances.

The use of the minimum volume problem for endmember identification is illustrated next. In general, we will call V the real values of endmembers defining simplex $S = conv(V)$ and use for the

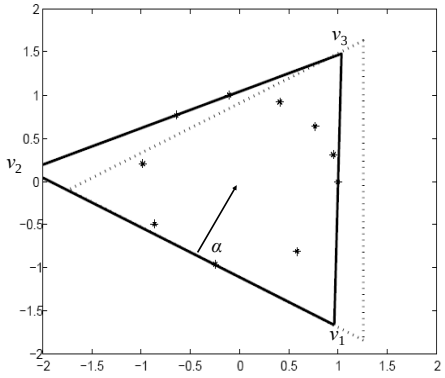

Figure 2 Enclosing 10 points on the unit ball. Dotted simplex is first guess as starting point of a local search agorithm with fixed line simplex as result

outer enclosing estimate $\hat{V}o$ and corresponding simplex $\hat{S}o$. In case all pixels would be convex combinations of (few) endmembers without any noise, the enclosing simplex $\hat{S}o$ obtains the endmembers V as vertices despite they do not appear in the pixels. Noise complicates the estimation. The bad case example instances show that the generic problem may have many optima. On the other hand in the specific case of unmixing, the pixels are spread well in the originating simplex and noise is low; the orientation of the simplex is more or less given. We will illustrate this in Example 3, where even not many pixels are present nor well spread. With many points, local non-global optima may exist, but they are close to the global one. Local nonlinear optimisation may generate good guesses of the endmembers and gives correct estimates if noise is absent.

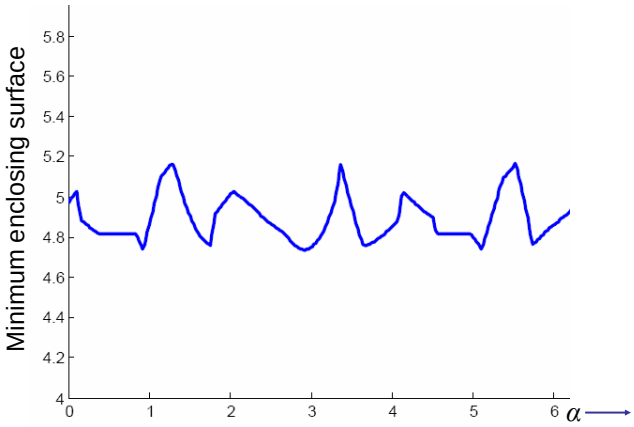

Figure 3 Minimum volume of enclosing simplex when fixing angle α of first edge

EXAMPLE 3. A matrix of endmembers is given by $V = \begin{pmatrix} 1 & 4 & 5 \\ 1 & 4 & 0 \end{pmatrix}$ depicted in Figure 4 as green dots and 20 pixels are generated as convex combinations depicted as crosses of which 10 are a combination of 2 endmembers and 10 a combination of 3. Only for a very low number of pixels enclosing simplex $\hat{S}o$ does not reflect matrix V as vertices. Simplex S has a volume of 15. We add

noise with $\sigma = 0.1$ and obtain the pixels in the rightmost picture of Figure 4. They are enclosed by a simplex $\hat{S}o$ with a volume of 17. Notice that less points are now located at the boundary. It may be intuitively clear that there should be at least 4 active points to obtain the minimum volume simplex in 2D.

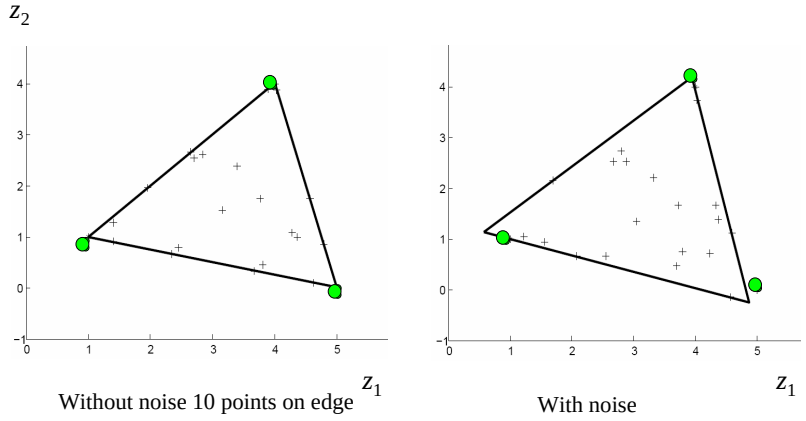

Figure 4 Three endmembers, 20 pixels in 2D with enclosing simplex $\hat{S}o$, with and without noise

If we intend to use the minimum volume formulation (3) and (4) to estimate the endmembers, noise will make the volume bigger. Like in regression, one would like to draw the bounding facets through the exterior of the cloud of points instead of enclosing it. In Section 4 a method is developed to deal with that.

Literature on spectral unmixing also uses a maximum volume simplex perspective (Winter (2003), Plaza et al. (2004)). The idea is that pure pixels representing the endmembers are present in the data set Z. Consider the pixel data now as a set $\mathbb{Z}$. One wants to find that subset $\mathbb{V}$ with $|\mathbb{V}| = n$ such that the corresponding simplex is of maximum volume. Using notation of sets and matrices, one can express this as

$$\max_{\mathbb{V}\subset\mathbb{Z}}\{f(V) := \det\begin{pmatrix} V \\ \mathbf{1}^T \end{pmatrix}\}, \tag{5}$$

where V is a matrix with the columns of $\mathbb{V}$. This defines a combinatorial optimization problem.

Use of the maximum volume problem does not guarantee that abundance is positive. However, the basic assumption is that the endmembers are present and that negative abundance simply may be caused by noise. We will call the estimate of V by maximum volume formulation (5) $\hat{V}i$ and the corresponding simplex $\hat{S}i$. N-FINDR is a heuristic algorithm that generates a (not necessarily optimal) solution of problem (5). We refer here to N-FINDR as an underlying algorithm and not to the commercial software that has been constructed around it.

EXAMPLE 4. Consider the setting of Example 3; 20 pixels are generated with a noise of $\sigma = 0.3$. Figure 5 gives minimum volume simplex $\hat{S}o$ with volume 18.5 enclosing the pixels and the maximum volume simplex $\hat{S}i$ with volume 11.25 where 3 pixels are selected out of 20, such that the resulting simplex has maximum volume.

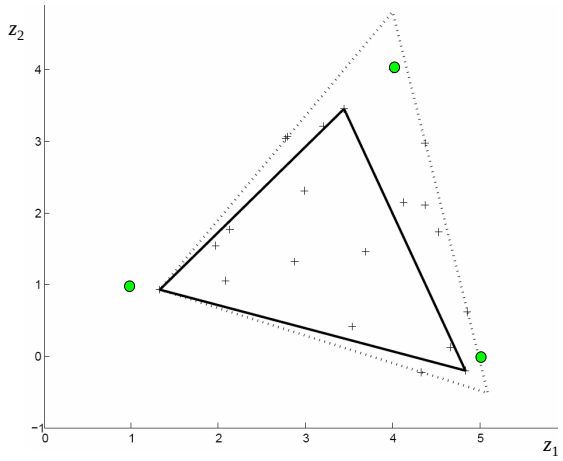

Figure 5 Maximum volume $\hat{S}i$ (solid line) and minimum volume $\hat{S}o$ (dotted line). Green dots are endmember values V and crosses are 20 noisy pixels z_k derived from them.

As illustrated by Example 4, the minimum enclosing simplex $\hat{S}o$ will always contain the maximum volume simplex $\hat{S}i$. However, there is no fixed relation with the simplex S determined by the real endmember spectra V that we intend to estimate. It may be clear that lower noise and more pixels as random combinations of the endmembers make $\hat{S}i$ go to S. Given fixed noise variance σ^2 and increasing the number of uniformly spread pixels, leads in limit to an overestimate of S, as observations fall outside S.

To determine the maximum volume estimate, problem (5) defines a combinatorial optimisation problem, where we select n pixels out of r. The number of possibilities grows as an n-degree polynomial in r. Usually, heuristic methods are used to find a good solution. The N-FINDR algorithm is a so-called local search heuristic in the context of literature on combinatorial optimisation, e.g. Aarts and Lenstra (1997). The algorithm has been extensively described in Plaza and Chang (2006), Plaza (2008) and Winter (2003) claims that under circumstances it converges to the optimum solution of problem (5). We will use a MATLAB implementation of the algorithm as a reference method to compare to the minimum volume procedure as described in Section 4.

4. Estimation procedure

As illustrated in the former sections, the minimum volume simplex $\hat{S}o$ gives an accurate estimate of the endmembers if noise is absent. That is, sufficiently many pixels should lay on the boundary of S. Mathematically, this means that abundance values $a_{j,k} = 0$ i.e. pixel k does not contain any constituent j. If pixels would have been generated uniformly over S, it is well known in literature on random sampling that with increasing dimension n, relatively more points have at least one abundance value close to zero; less points can be found in the interior of the simplex, see e.g. Hendrix and Toth (2010). However, we are not interested in completely randomly generated pixels, but in spectral images. In that area, it is known that in reality a pixel spectrum consists of a mix of at most 4–5 constituents. Reasoning the other way around, at least $n-5$ values $a_{j,k} = 0$ for each pixel.

Why is the latter of any importance? As soon as noise is added, one can approximate with probability theory the chance ρ that a pixel lays inside S. Let N abundance values of pixel k be 0. For each element with a value of zero, the probability after adding noise that the observation of $\hat{a}_{j,k}$

of the abundance value is positive is taken as $\frac{1}{2}$. The probability the observation $\hat{a}_k$ of the pixel is inside S is at most

$$p_N = \left(\frac{1}{2}\right)^N. \tag{6}$$

This is not completely correct. Given model (2) and estimator (4)

$$\hat{a} = a + \begin{pmatrix} V \\ \mathbf{1}^T \end{pmatrix}^{-1} \begin{pmatrix} \xi \\ 1 \end{pmatrix} \tag{7}$$

such that one should consider the probability mass of the corresponding positive orthant of $\hat{a}$. Equation (6) gives an approximation for all abundance vectors with N zeros. Moreover, we say "at most", because also low values of $a_{j,k}$ may yield observations outside S. Therefore it is relevant that in realistic images the noise is relatively low and real abundance (positive value) is at least noticed. We want to estimate the number of observations $P = \rho \times r$ located inside simplex S. This number depends on the distribution of zero abundance values over the pixels (without noise). Let r_N denote the number of pixels that have N zero values $N = 0, 1, \ldots, n-1$ such that $\sum r_N = r$. The number of pixels inside S is at most

$$P = \sum_{N=0}^{n-1} r_N p_N. \tag{8}$$

Of course in real images the distribution is unknown. However, with synthetic data one can experiment with these proportions. The relevance of P is that an outer approximation $\hat{So}$ of S should in fact ignore the $r - P$ pixels outside S and enclose the P that are located in S. But how to know which ones are in and which ones are out? This consideration is the basis of a new estimation algorithm.

4.1. Estimate $\hat{V}$ of endmember matrix V

The idea is to base the final estimate of endmembers on the $\rho = \frac{P}{r}$ fraction of pixels that we expect to be interior with respect to S. Iteratively the endmembers are estimated from the minimum volume problem and the active pixels at its boundary are removed up to a ρ fraction is left over. We start with an initial simplex that does not enclose the points, but has an orientation in the same way if one repeats the algorithm with the same instance. To obtain a starting simplex V, we take the

Algorithm 1 : MINVEST

Inputs: Z: $(n-1) \times r$ matrix of pixel scores
ρ: percentage of interior pixels
Outputs: V: $(n-1) \times n$ matrix of endmembers
Funct MinVol estimator

1. $Z0 := Z$, R: number of pixels in $Z0$, generate starting simplex V
2. **while** $(R > \rho r)$
3. Generate V by solving (3) and (4) for $Z0$, former V is starting value
4. remove active pixels at boundary $conv(V)$ from $Z0$, update R
5. **endwhile**

extreme values of the cloud defined by Z setting first:

$$V_{i,j} = \min_k z_{i,k} \quad i = 1, \ldots, n-1, j = 1, \ldots, n \tag{9}$$

and further

$$V_{i,i+1} = \max_k z_{i,k} \quad i = 1, \ldots, n-1. \tag{10}$$

EXAMPLE 5. Given the simplex of endmembers of Example 3 we are going to estimate with the new algorithm. $r = 100$ pixels are generated on its boundary, such that they have one zero abundance value each. After adding noise (we take $\sigma = 0.2$), at least half of the pixels is located outside; we take $\rho = 0.5$. One can observe the starting simplex which is parallel to the axes given by a dashed line in Figure 6. We use the FMINCON routine to generate the enclosing minimum volume simplices $\hat{So}$, dotted lines. About 6 points are active and removed from the set of pixels. $\hat{So}$ is determined again using the former estimate as starting value. This process proceeds up to the final estimate in this case is based on 56 pixels. The estimated matrix of endmembers is given by $\hat{V} = \begin{pmatrix} 1.02 & 5.03 & 4.00 \\ 1.03 & -0.02 & 4.26 \end{pmatrix}$ with a volume of 16.07 and its simplex is depicted by a solid line in Figure 6.

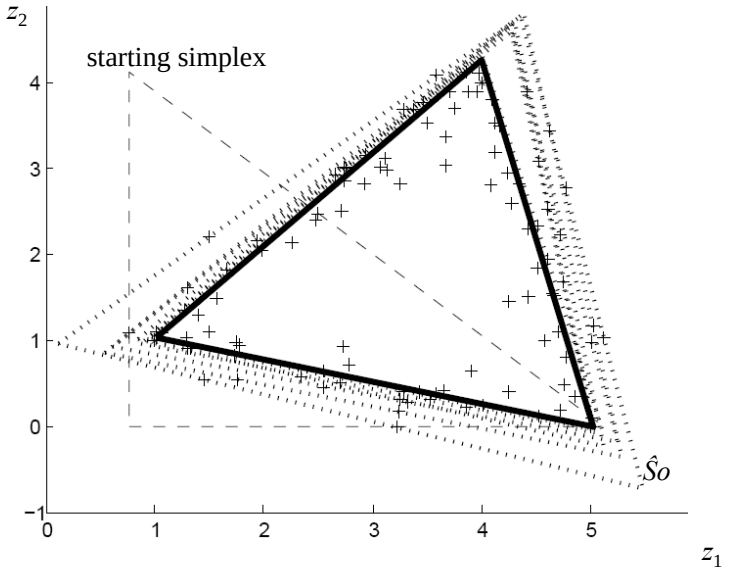

Figure 6 Iterative estimates of S

4.2. Estimate $\hat{A}$ of abundance matrix A

To recover the abundance values from the estimated endmembers V the term *linear spectral unmixing* (LSU) is used when nonnegativeness of estimated abundance is not taken into account. In the space of scores this can be done by calculating

$$A = \begin{pmatrix} V \\ \mathbf{1}^T \end{pmatrix}^{-1} \begin{pmatrix} Z \\ \mathbf{1}^T \end{pmatrix}. \tag{11}$$

For the fraction of pixels located in the final set $Z0$ or geometrically within simplex $\hat{S}$ we have automatically positive abundance values. For pixels z_k outside $\hat{S}$, we have at least one corresponding $a_{jk} < 0$. The term *fully constrained linear spectral unmixing* (FCLSU) is used if we want to force abundance values to be nonnegative (Heinz and Chang (2001)). One way to do so is described here.

With the idea that the noise of z_k is componentwise independent we choose to project z_k on the facet of $\hat{S}$ closest to z_k and determine the abundance for the endmembers in the plane of that facet. This can be done by determining the endmembers v_j in the facet corresponding to $a_j > 0$ and

putting them in a selection matrix U. After constructing a matrix W which gives the directions in the plane of the facet with columns $w_j = u_j - u_1$, the abundance can be derived from the projection coefficients $b = (W^T W)^{-1} W^T z$ as outlined in Algorithm 2. In the result of Example 5, Figure 7

Algorithm 2 : abundance

Inputs: V: $(n-1) \times n$ matrix of endmember scores
z: $n-1$ vector of pixel scores
Outputs: a: nonnegative vector of abundance
Funct Abund estimator

1. Determine a via (4)
2. **while** not $(a \geq 0)$
3. Select v_j with $a_j > 0$ and put into matrix U
4. make spanning matrix W with columns $w_j := u_{j+1} - u_1$
5. determine projection coefficients $b := (W^T W)^{-1} W^T z$
6. abundance a_j corresponding to u_k is b_k
7. abundance a_j corresponding to u_1 is $1 - \sum b_k$
8. for $a_j < 0$, $a_j := 0$
9. **endwhile**

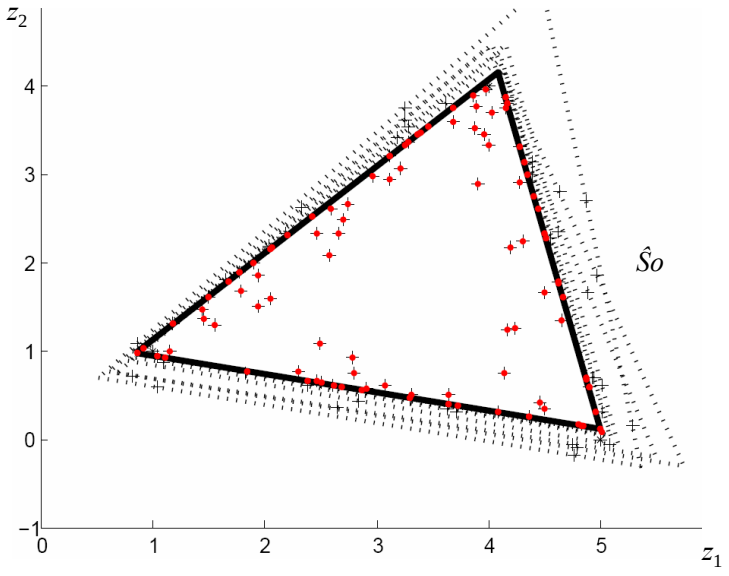

Figure 7 Estimates of S and the interior and projected pixels in red

shows interior pixels and projected versions of outside pixels by red dots as a result of Algorithm 2.

5. Computer simulated data experiments

In this section, we use computer simulations in order to test the accuracy of MINVEST in comparison to another popular endmember extraction method, N-FINDR, in a controlled setting. The reason for using simulations is that all details of the scenario are known. Consequently, they can be systematically investigated. We develop several experiments, where the first two experiments represent simple examples in which the advantages of MINVEST over methods that assume the presence of pure pixels in the scene (such as N-FINDR) are illustrated graphically. Then, we perform experiments using a computer simulated hyperspectral scene constructed from real spectral observations.

To measure the performance, one should define the exact performance indicator. The quality of estimation $\hat{V}$ of V is measured as the standard deviation estimate assuming $\hat{V}$ is unbiased also called root mean squared error (RMSE):

$$\sigma_V = \sqrt{(\frac{1}{n(n-1)} \sum_i \sum_j (\hat{V}_{ij} - V_{ij})^2)}. \tag{12}$$

The quality of estimation $\hat{A}$ of A is measured as standard deviation (RMSE):

$$\sigma_A = \sqrt{(\frac{1}{r(n-1)} \sum_i \sum_k (\hat{A}_{ik} - A_{ik})^2)}. \tag{13}$$

To distinguish, we will use σ_A if $\hat{A}$ is generated by linear spectral unmixing (11) and σ_{Ap} if $\hat{A}$ is generated by the procedure described to generate FCLSU-based abundances.

Table 1 Standard deviation estimates (RMSE) of endmembers V and abundance A obtained by N-FINDR and MINVEST algorithms given noise σ.

	N-FINDR					MINVEST				
σ	0.01	0.1	0.2	0.5	0.7	0.01	0.1	0.2	0.5	0.7
σ_V	.030	.118	.233	.857	1.359	.013	.111	.194	.486	.922
σ_A	.011	.063	.114	.259	.323	.007	.058	.105	.204	.266
σ_{Ap}	.008	.048	.092	.224	.281	.005	.048	.086	.174	.234

5.1. Small experiment

Our research question in this experiment is: How good can a method reproduce the endmembers V and the abundance matrix A? To test this we build a small experiment with the following ingredients:

- The case has $n = 5$ endmembers and $r = 500$ pixels.
- The endmember matrix to be estimated is fixed on $V = \begin{pmatrix} 0 & 1 & 2 & 3 & 5 \\ 5 & 1 & 3 & 5 & 4 \\ 0 & 1 & 1 & 2 & 0 \\ 0 & 0 & 2 & 1 & 0 \end{pmatrix}$. We keep the order of endmembers fixed by sorting the first row. In this way, estimate $\hat{V}$ and V are easily compared.
- To mimic the idea of combinations of a few constituents, a ground truth abundance matrix A is generated consisting for 50% of mixtures of 2 endmembers and for 50% of mixtures of 3 endmembers.
- The input score matrix Z is taken as $Z = VA + \sigma \times \xi$, with ξ generated standard white noise.
- The value of the parameter ρ can be derived from the experimental data; $\rho = 18.25\%$.
- Given that the performance indicators depend on (pseudo-)randomly drawn white noise, we replicate for each generated matrix A, i.e. generate replications for Z, and take the average of the measures. For each ground-truth matrix A we replicated white noise 100 times.

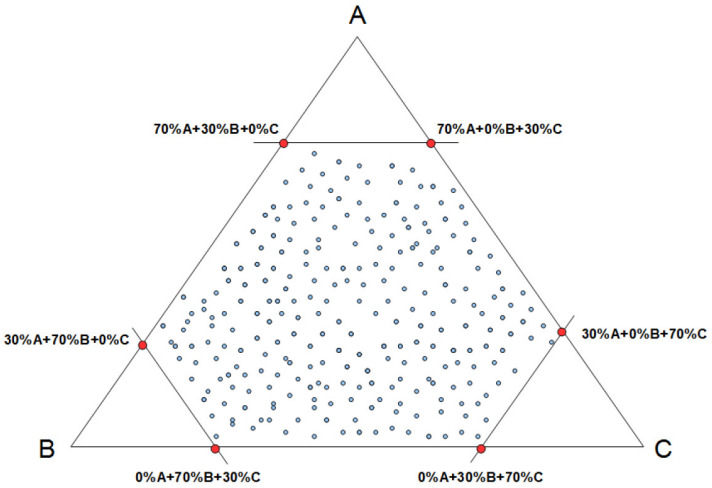

Figure 8 Toy data set without pure pixels.

The measured performance for N-FINDR and MINVEST is given in Table 1. It shows standard deviation estimates σ_V of endmembers, σ_A of fractional abundances calculated via (11) and σ_{Ap} via FCLSU. One can observe in Table 1 that the standard deviation of the estimates is in the same order of magnitude as that of noise. This means that the procedures give results as accurate as the input data. Deviation of endmembers and abundances estimations provided by N-FINDR are higher than those obtained with MINVEST.

5.2. Scenario without pure pixels

The presence of pure pixels in a hyperspectral image is rare due to several reasons, such as the available spatial resolution of imaging spectrometers, typically various meters per pixel (Green et al. (1998)). This compromises the assumption that pure pixels should be present in the original scene adopted by algorithms such as N-FINDR. In this subsection, we illustrate graphically the advantages of MINVEST over N-FINDR in this kind of instances, which is typical in practice due to such spatial resolution considerations. We generated a toy data set which is illustrated graphically in Figure 8.

As shown in Figure 8, the simulated data set does not include any pure pixels, and the mixtures y_k of the three endmembers designated as 'A', 'B' and 'C' have a maximum degree of purity of 70% of an endmember. So, although the pure observations 'A', 'B' and 'C' have been used to create the simulated mixtures, they are not included in the data to be processed. As a result, finding the endmembers in this toy example is a challenging problem.

Fig. 9(a) shows a representation of the simulated data set in two dimensions, obtained by representing the scores z_k of the first two principal components. Since the mixtures are formed using three endmembers (designated as 'A', 'B' and 'C'), the goal is to find a simplex formed by three vertices that can enclose all the observations. Figure 9(b) shows the endmembers found by MINVEST (red color) and by N-FINDR (green color) after applying both algorithms to the data set in Figure 9(b). The N-FINDR algorithm selects real observations i.e., pixels present in the data, as endmembers, while the MINVEST algorithm selects endmembers which are not present. The corresponding simplices are given in Figure 9(c). One can observe that the endmembers produced by MINVEST are almost identical to the ground-truth endmembers used to construct the data, defining a simplex (red color) that includes all observations. However, the endmembers extracted by N-FINDR from real observations cannot enclose all other observations, resulting in negative fractional abundance estimations for those observations not included in the simplex (green color).

This simple but revealing example illustrates the advantages of using minimum enclosing volume-based approaches over maximum volume-based approaches when pure observations are not present

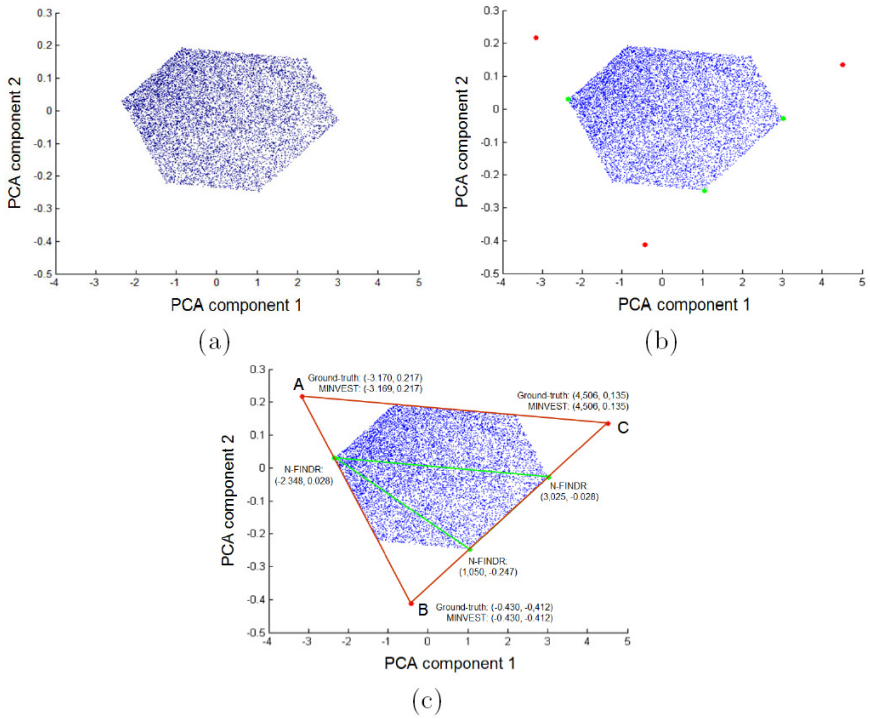

Figure 9 (a) Two-dimensional representation of the toy data set without pure pixels. (b) Endmembers extracted by MINVEST (red) and N-FINDR (green). (c) Coordinates of the endmembers and simplices defined by the endmembers extracted by MINVEST (red) and N-FINDR (green).

in the input hyperspectral data set, a common situation in practice given sensor spatial resolution considerations. Further experiments are required to compare both types of approaches when pure pixels are present in the input hyperspectral data.

5.3. Scenario with pure pixels

In this experiment, the reflectance spectra of five U.S. Geological Survey (USGS) ground-truth mineral spectra (alunite, buddingtonite, calcite, kaolinite and muscovite) have been managed for computer simulations. All signatures are available online[1] and have been used to simulate a square synthetic image scene with a size of 100×100 pixels. Mixtures of the five endmembers have been simulated based on ground-truth fractional maps constructed so that the endmembers are located at the four corners and at the center of the image, and signature abundance decreases linearly away from the pure pixels, a simulation scenario already considered in Plaza et al. (2004). Gaussian noise with a signal-to-noise ratio (SNR) ranging from $30:1$ to $110:1$ was added to the scene to simulate contributions from ambient (clutter) and instrumental sources.

Figure 10(a) shows ground-truth fractional abundance maps compared with the maps obtained by MINVEST for the simulated image without noise in Figure 10(b) and with an SNR of 30:1 in Figure 10(c). As shown, the visual appearence of the fractional abundance maps obtained after using the MINVEST algorithm is in very good compromise with the ground-truth fractional abundance maps, even for a scenario with high noise. It should be noted that the estimated fractional abundance maps are always highly correlated in terms of the spatial distribution of abundances in the fractional maps with regards to the corresponding ground-truth maps.

Figure 11 displays the fractional abundance estimations obtained by N-FINDR combined with the FCLSU algorithm for abundance estimation. It can be observed that the use of N-FINDR endmembers

[1] http://speclab.cr.usgs.gov/spectral-lib.html

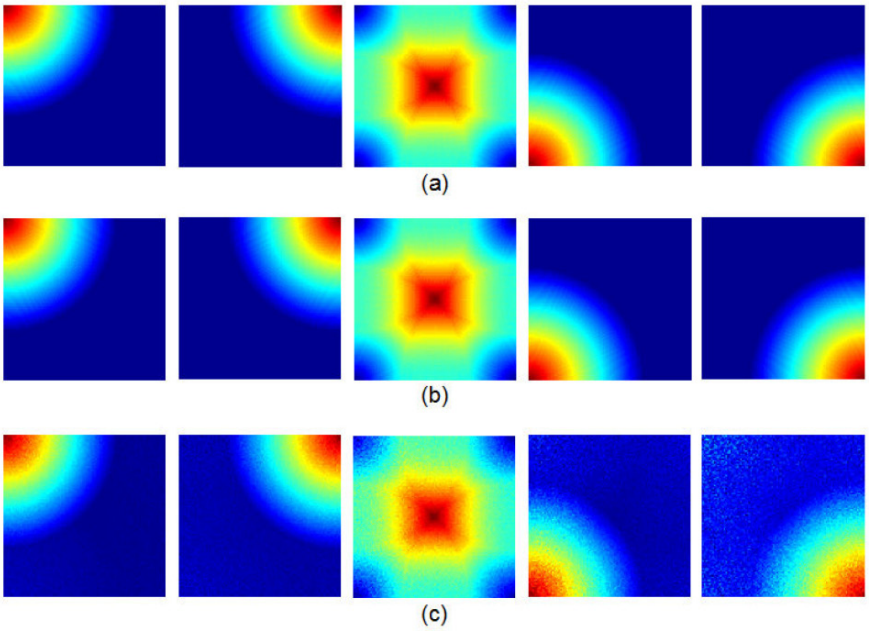

Figure 10 (a) Ground-truth fractional abundance maps. (b) Fractional abundance estimations for the simulated image without noise using MINVEST algorithm. (c) Fractional abundance estimations for the simulated image with SNR of 30:1 using MINVEST algorithm.

resulted in fractional maps which are not as properly distributed (in spatial terms) as those provided by MINVEST. In particular, this is the case for the simulated scene with SNR of 30:1 in Figure 11(c). Despite the fact that the estimations resulting from N-FINDR appear less similar, visually, to those in Figure 11(a), an investigation in terms of the RMSE of the estimated abundance fractions with regards to the true ones is needed in order to substantiate if there are any scaling issues involved as was the case for some of the MINVEST estimations.

Table 2 RMSE values that compare the fractional abundances estimated by different methods with the true abundance fractions using simulated scenes with different SNRs

SNR	MINVEST	N-FINDR
∞	0.0000	0.0020
110	0.0172	0.0039
90	0.0206	0.0053
70	0.0262	0.0067
50	0.0347	0.0117
30	0.0522	0.0331

Table 2 gives the RMSE between the fractional abundance maps estimated for the endmembers extracted using N-FINDR (combined with FCLSU) and MINVEST. As shown by Table 2, the best estimations for the simulated scene without noise are provided by MINVEST, while the best estimations for the scenes with simulated noise are provided by N-FINDR. This seems not to be consistent with the visual appearance of the fractional abundance maps estimated by the different methods, in particular for the maps displayed in Figure 11(c) and their visual agreement with the ground-truth maps. However, this is merely a scaling issue. Due to the dependence of MINVEST on a parameter ρ that gives the number of pixels fallen inside the original simplex, the estimate may over or underestimate its volume. This means that all abundance values are either too big or too small resulting in a

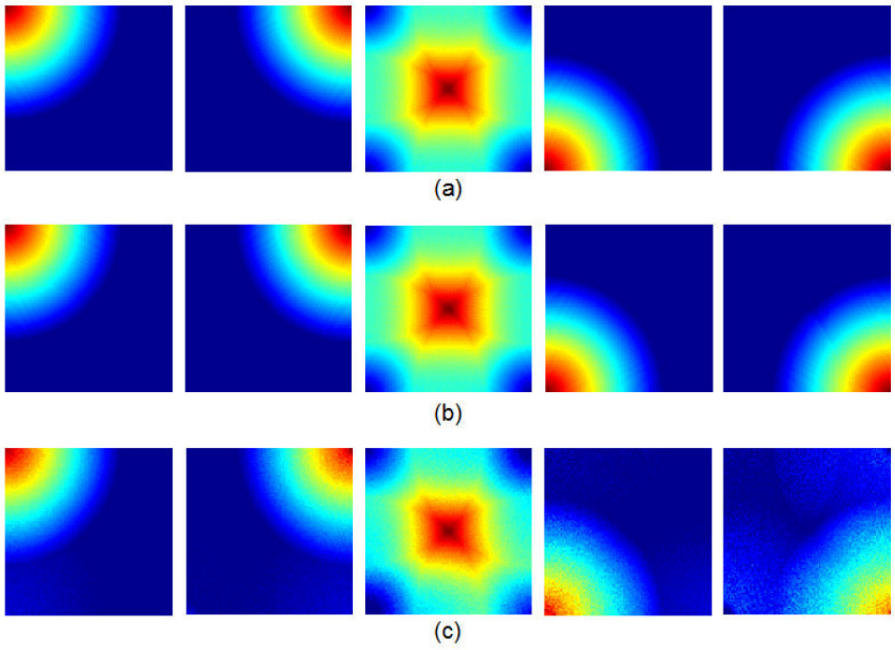

Figure 11 (a) Ground-truth fractional abundance maps. (b) Fractional abundance estimations for the simulated image without noise using N-FINDR algorithm followed by FCLSU. (c) Fractional abundance estimations for the simulated image with SNR of 30:1 using N-FINDR algorithm followed by FCLSU.

higher RMSE value. The visual correspondance (correlation) tells us that apparently the orientation of the generated simplex by MINVEST is better than that generated by N-FINDR. The scaling issue should be further investigated in future work in order to establish a better correspondence between the MINVEST estimations and the ground-truth maps in Figure 10(a) and thus confirm the good visual impression provided by the MINVEST-derived fractional maps.

6. Conclusions

We explored the possibility of using the minimum volume simplicial enclosure problem as a basis for a new algorithm called MINVEST for joint endmember extraction and spectral unmixing and found the following results.

- The problem of unmixing hyperspectral data may be a hard to solve problem.
- The minimum volume simplicial enclosure problem is a Global Optimization problem where the number of optima depends in worst case on the number of points in the convex hull of the instance.
- The resulting simplex of the (combinatorial) maximum volume simplex problem is enclosed in the result of the minimum volume enclosing simplex problem.
- Local search from a good starting simplex leads in general to the global optimum for the case of spectral unmixing due to well spread data in the originating simplex and low noise in practice.
- The new MINVEST algorithm does not require pure pixels to be present in the scene of the instance unlike the N-FINDR and other similar endmember extraction algorithms.
- In the case that there is no noise and we have well spread data over the boundary of the spectral simplex, MINVEST successfully recovers the original endmembers and ground truth abundances.
- The root mean squared error perfomance indicator is sensitive to scaling in its use for measuring abundance discrepancies.
- The results of MINVEST seem more correlated to ground truth abundance data than the ones of N-FINDR.

Further research can focus on the relation between the used values for parameter ρ (the estimated fraction of points in the originating simplex) and the scaling effects observed in the abundance measure. A detailed investigation of computational complexity and possible parallelization strategies for the discussed methods is also a topic deserving future research.

References

Aarts, E. H. L. and Lenstra, J. K. (1997). *Local Search Algorithms*. Wiley, New York.

Adams, J. B., Smith, M. O., and Johnson, P. E. (1986). Spectral mixture modeling: a new analysis of rock and soil types at the Viking Lander 1 site. *Journal of Geophysical Research*, 91:8098–8112.

Chan, T., Chi, C., Huang, Y., and Ma, W. (2009). Convex analysis based minimum-volume enclosing simplex algorithm for hyperspectral unmixing. In *Proceedings of the 2009 IEEE international conference on Acoustics, Speech and Signal Processing*, pages 1089–1092. IEEE, Piscataway.

Chang, C.-I. (2003). *Hyperspectral Imaging: Techniques for Spectral Detection and Classification*. Kluwer Academic/Plenum Publishers: New York.

Craig, M. (1994). Minimum-volume transforms for remotely sensed data. *IEEE Transactions on Geoscience and Remote Sensing*, 32(3):542–552.

Goetz, A. F. H., Vane, G., Solomon, J. E., and Rock, B. N. (1985). Imaging spectrometry for Earth remote sensing. *Science*, 228:1147–1153.

Green, R. O., Eastwood, M. L., Sarture, C. M., Chrien, T. G., Aronsson, M., Chippendale, B. J., Faust, J. A., Pavri, B. E., Chovit, C. J., Solis, M., et al. (1998). Imaging spectroscopy and the airborne visible/infrared imaging spectrometer (AVIRIS). *Remote Sensing of Environment*, 65(3):227–248.

Heinz, D. and Chang, C. (2001). Fully constrained least squares linear spectral mixture analysis method for material quantification in hyperspectral imagery. *IEEE Transactions on Geoscience and Remote Sensing*, 39:529–545.

Hendrix, E. M. T. and Toth, B. G. (2010). *Introduction to Nonlinear and Global Optimization*. Springer, Cambridge.

Keshava, N. (2003). A survey of spectral unmixing algorithms. *Lincoln Laboratory Journal*, 14:55–78.

Keshava, N. and Mustard, J. F. (2002). Spectral unmixing. *IEEE Signal Processing Magazine*, 19(1):44–57.

Khachiyan, L. and Todd, M. (1993). On the complexity of approximating the maximal inscribed ellipsoid for a polytope. *Mathematical Programming*, 61:137–159.

Miao, L. and Qi, H. (2007). Endmember extraction from highly mixed data using minimum volume constrained nonnegative matrix factorization. *IEEE Transactions on Geoscience and Remote Sensing*, 45:765–777.

Plaza, A. and Chang, C.-I. (2006). Impact of initialization on design of endmember extraction algorithms. *IEEE Transactions on Geoscience and Remote Sensing*, 44(11):3397–3407.

Plaza, A., Martinez, P., Perez, R., and Plaza, J. (2004). A quantitative and comparative analysis of endmember extraction algorithms from hyperspectral data. *IEEE Transactions on Geoscience and Remote Sensing*, 42(3):650–663.

Plaza, J. (2008). *Procesamiento paralelo de imagenes hiperspectrales utilizando arquitecturas de computacion neuronal*. PhD thesis, Universidad de Extremadura, Caceres.

Richards, J. A. and Jia, X. (2006). *Remote Sensing Digital Image Analysis: An Introduction*. Springer.

Sun, P. and Freund, R. (2004). Computation of minimum-volume covering ellipsoids. *Operations Research*, 52(5):690–706.

Winter, M. E. (2003). N-FINDR: An algorithm for fast autonomous spectral end-member determination in hyperspectral data. *Proc. SPIE Image Spectrometry V*, 3753:266–277.

Zhou, Y. and Suri, S. (2002). Algorithms for a minimum volume enclosing simplex in three dimensions. *SIAM Journal on Computing*, 31(5):1339–1357.